

Dark Matter production during Warm Inflation via Freeze-In

Katherine Freese,^{1,2,3,*} Gabriele Montefalcone,^{1,†} and Barmak Shams Es Haghi^{1,‡}

¹*Texas Center for Cosmology and Astroparticle Physics,
Weinberg Institute for Theoretical Physics, Department of Physics,
The University of Texas at Austin, Austin, TX 78712, USA*

²*The Oskar Klein Centre, Department of Physics,
Stockholm University, AlbaNova, SE-10691 Stockholm, Sweden*

³*Nordic Institute for Theoretical Physics (NORDITA), 106 91 Stockholm, Sweden*

We present a novel perspective on the role of inflation in the production of Dark Matter (DM). Specifically, we explore the DM production during Warm Inflation via ultraviolet Freeze-In (WIFI). We demonstrate that in a Warm Inflation (WI) setting the persistent thermal bath, sustained by the dissipative interactions with the inflaton field, can source a sizable DM abundance via the non-renormalizable interactions that connect the DM with the bath. Compared to the (conventional) radiation-dominated (RD) UV freeze-in scenario for the same reheat temperature (after inflation), the resulting DM yield in WIFI is always enhanced, showing a strongly positive dependence on the mass dimension of the non-renormalizable operator. Of particular interest, for a sufficiently large mass dimension of the operator, the entirety of the DM abundance of the Universe can be created during the inflationary phase. For the specific models we study, we find an enhancement in DM yield of up to 30 orders of magnitude relative to RD UV freeze-in for the same reheat temperature. Our findings also suggest a broader applicability for producing other cosmological relics, which may have a substantial impact on the evolution of the early Universe.

Introduction. — In spite of overwhelming evidence for dark matter (DM) which is based on its gravitational effects, the nature of DM remains unknown. In consideration of the origin of DM and also DM searches, the possible non-gravitational interactions of DM are strongly motivated. An intriguing mechanism to produce DM is through interaction with a thermal bath. Depending on the non-gravitational interactions between DM and the bath, the DM abundance can be established mainly by freeze-out or freeze-in mechanisms.

In freeze-out, the DM interaction with the thermal bath is strong enough to keep DM in chemical equilibrium with the bath at early times, and its eventual departure from chemical equilibrium sets the final DM abundance. In freeze-in, on the contrary, the DM interacts with the thermal bath so weakly that it never comes to thermal equilibrium, and the DM final abundance is built up gradually over time [1]. The suppressed interaction between DM and the thermal bath, characteristic of the freeze-in mechanism, can be due to renormalizable interactions with a very small coupling constant, known as infrared (IR) freeze-in [1], or because of non-renormalizable interactions with a heavy mass scale, known as ultraviolet (UV) freeze-in [2]. While in IR freeze-in the DM abundance is set by the (low) temperature near the DM mass (i.e. the IR physics), in the UV freeze-in case, the abundance of DM is (typically) sensitive to the highest temperature of the bath.¹ Therefore, any possible evolution

of the radiation bath prior to the radiation dominated (RD) era, basically can affect the DM abundance from UV freeze-in. Previous work has studied the effects of a radiation bath on DM production in the intermediate era after inflation but before radiation domination. For example, it is known that after inflation and during reheating, provided rapid thermalization, the bath produced by the early inflaton decay can achieve temperatures much higher than the reheat temperature evaluated based on the instantaneous decay of the inflaton [3–5]. Careful consideration [6, 7] of the UV freeze-in of DM during reheating, within a matter domination era, has shown that the DM yield can be enhanced compared to the case of instantaneous reheating. This result has also been generalized to transitions from other non-standard cosmologies to the RD era [8, 9]. The impact of non-thermal effects during reheating on DM yield has also been considered in Ref. [10].

All existing studies to date of DM production via UV freeze-in have primarily focused on the physics of reheating, implicitly assuming that any amount of DM that may have been produced during the inflationary expansion was diluted away. This however may not be the case. It is in fact possible for a persistent thermal bath to exist throughout the inflationary epoch, continually generated by dissipative interactions with the inflaton field. This is known as the warm inflation (WI) scenario [11–13] and, as we will show in this *letter*, it emerges as a natural framework for the efficient production of DM via freeze-in during the period of inflationary expansion. Assuming no direct coupling between DM and the inflaton field, the persistent radiation bath can source a sizable DM abundance via the non-renormalizable interaction characteristic of UV freeze-in, without spoiling the inflaton dynamics. To encapsulate this novel framework, where

* ktfreese@utexas.edu

† montefalcone@utexas.edu

‡ shams@austin.utexas.edu

¹ For the case studied in this *letter*, we will find a different dependence for the DM abundance, see Eq. (7).

DM is produced through UV freeze-in concurrently with the WI phase, we introduce the acronym WIFI, standing for ‘Warm Inflation Freeze-In’.

We find that in WIFI, the DM yield is enhanced remarkably compared to the conventional UV freeze-in yield from a RD era at the same reheat temperature. Specifically, as the mass dimension of the non-renormalizable operator increases, so does the enhancement; with the majority of the DM yield being generated during inflation for the case where the mass dimension is sufficiently large. This outcome represents the pivotal contribution of our work which establishes, for the first time, a consistent framework in which the primordial accelerated expansion is central in determining the thermal DM production via freeze-in.

General Setup.— In WI, the energy density of the inflaton field is continuously transferred to a thermal bath through dissipative effects. The radiation persists and eventually dominates the energy density of the Universe. This provides a smooth transition from the inflationary phase to the RD one which alleviates the need for a separate reheating process.

In WIFI, while the inflaton field is in thermal equilibrium with the radiation bath, it does not interact with the DM candidate. The DM, which has a mass less than the temperature of the bath, interacts with the radiation via a non-renormalizable interaction suppressed by some powers of a mass scale, e.g. the mass of a heavy mediator, larger than the temperature of the bath. The suppressed interaction between the DM and the bath makes DM a harmless addition to the WI framework. The evolution of the background homogeneous inflaton field ϕ in the presence of a thermal bath at temperature T is:

$$\ddot{\phi} + (3H + \Upsilon)\dot{\phi} + dV(\phi)/d\phi = 0, \quad (1)$$

$$\dot{\rho}_r + 4H\rho_r = \Upsilon\dot{\phi}^2, \quad (2)$$

$$H^2 = (\rho_\phi + \rho_r) / (3M_{\text{pl}}^2), \quad (3)$$

where $\rho_\phi = V(\phi) + \dot{\phi}^2/2$ and $\rho_r = (\pi^2/30)g_*(T)T^4$ indicate the energy density of the inflaton field and radiation, respectively, $g_*(T)$ counts the total number of relativistic degrees of freedom, and $M_{\text{pl}} \equiv 1/\sqrt{8\pi G} \approx 2.4 \times 10^{18}$ GeV is the reduced Planck mass. The dissipation term, $\Upsilon(\phi, T)$, describes the rate at which the energy in the inflaton field converts into radiation and its exact form depends on the underlying microphysical model [13].

The evolution of the number density of DM, χ , denoted by n_χ , is governed by the Boltzmann equation:

$$\dot{n}_\chi + 3Hn_\chi = T^{2n+4}/\Lambda^{2n}, \quad (4)$$

where Λ is the cutoff of the effective field theory which describes the interaction between DM and the radiation, and represents, for example, the mass of a heavy mediator that couples DM to the bath. This effective interaction is expressed as an operator of mass dimension $n+4$ for $n \geq 1$, i.e. $\mathcal{L} \supset \mathcal{O}_{n+4}/\Lambda^n$ [2], and remains applicable

as long as $T < \Lambda$.² In freeze-in, the DM never reaches thermal equilibrium with the bath, therefore the backreaction of χ ’s annihilation on radiation is neglected. Since, $\rho_\chi \ll \rho_r$, the contribution of DM in Eqs. (2) and (3) is safely ignored.

Recasting Eq. (4) in terms of the DM yield, $Y_\chi \equiv n_\chi/s$, with $s = (2\pi^2/45)g_{*,S}(T)T^3$ being the entropy density of the thermal bath,³ leads to the following solution:

$$Y_\chi(N_e) = \frac{45}{2\pi^2 g_*} \frac{e^{-3N_e}}{T^3(N_e)} \int_{N_{e,0}}^{N_e} \mathcal{I}_\chi(N'_e) dN'_e, \quad (5)$$

where

$$\mathcal{I}_\chi(N_e) \equiv e^{3N_e} \frac{T^{2n+4}(N_e)}{\Lambda^{2n} H(N_e)}, \quad (6)$$

and N_e is the number of e-folds defined by $dN_e \equiv H dt$. A vanishing DM yield at some initial time, $N_{e,0}$, is assumed. It is worth mentioning that \mathcal{I}_χ is the rate of change of the comoving DM number density, $N_\chi \equiv e^{3N_e} n_\chi$, i.e. $\mathcal{I}_\chi = dN_\chi/dN_e$.

According to Eq. (5), which is applicable to UV freeze-in within any cosmology, the DM yield depends on the evolution of $T(N_e)$ and $H(N_e)$. In a WI setting, these functions can be evaluated simply from the set of Eqs. (1), (2), and (3). Therefore, the DM yield evolution is clearly contingent on the precise details of the WI model under consideration (e.g. the inflaton potential, the form of the dissipation rate, etc.). Nevertheless, we can still extract overarching conclusions about the DM relic abundance within our framework. In fact, $\mathcal{I}_\chi(N_e)$ (Eq. (6)) is generically an exponentially increasing function through most of the inflationary phase, when $\rho_\phi \gg \rho_r$, and it becomes an exponentially decreasing function shortly after the end of inflation at the onset of the RD phase, when $\rho_\phi \ll \rho_r$. It can, therefore, be argued that the function $\mathcal{I}_\chi(N_e)$, or equivalently, the rate of production of the comoving DM number density, is sharply peaked at some e-fold, N_e^{peak} , which is the solution of $d\mathcal{I}_\chi(N_e)/dN_e = 0$, i.e.,

$$3 + (2n + 4) \frac{d \ln T(N_e)}{dN_e} - \frac{d \ln H(N_e)}{dN_e} = 0. \quad (7)$$

This allows us to estimate the DM yield at late times, i.e. for $N_e > N_e^{\text{peak}}$, by using the peak value of \mathcal{I}_χ , to obtain:

$$Y_\chi(N_e) \simeq \frac{45}{2\pi^2 g_*} \frac{e^{3(N_e^{\text{peak}} - N_e)}}{\Lambda^{2n} T^3(N_e)} \Delta N_e^{\text{peak}} \times \frac{T^{2n+4}(N_e^{\text{peak}})}{H(N_e^{\text{peak}})}, \quad (N_e > N_e^{\text{peak}}), \quad (8)$$

² Depending on the details of the interaction between the DM and the bath as well as the nature of DM (e.g., the number of internal degrees of freedom for the DM) one may have to multiply the source term (the right hand side of Eq. (4)) by a numerical prefactor; here, since the same factor would arise in the conventional RD scenario, we set this to unity.

³ We assume that $g_{*,S}(T) = g_*(T)$ and $dg_*(T)/dT = 0$.

where ΔN_e^{peak} , denoting the full width at half maximum of \mathcal{I}_χ , always exceeds 1 and typically encompasses an interval of a few e-folds. To better understand the importance of this result, one can compare it with the final yield of DM produced from UV freeze-in (Eq. (4)) in a RD epoch which starts at some initial time $N_{e,0}$ with temperature $T(N_{e,0}) = T_{\text{rh}}$. In a RD era, conservation of entropy results in $T(N_e) = T_{\text{rh}} e^{(N_{e,0} - N_e)}$, which together with $H(N_e) \sim T^2(N_e)/M_{\text{Pl}}$, and Eqs. (5) and (6) give rise to following final yield for the DM:

$$Y_{\chi,\infty}^{\text{RD}}(T_{\text{rh}}) \simeq \frac{1}{\sqrt{2}} \left(\frac{45}{\pi^2 g_*} \right)^{3/2} \frac{1}{2n-1} \frac{M_{\text{Pl}} T_{\text{rh}}^{2n-1}}{\Lambda^{2n}}. \quad (9)$$

While the yield of the DM in UV freeze-in from a RD era depends on the highest temperature, i.e. T_{rh} , and freezes in very quickly to its final value, in the WI scenario, the bulk of it is produced at N_e^{peak} , given by Eq. (7).

Since in WIFI, DM production starts from the beginning of the inflation and always peaks before the onset of the RD phase (potentially even before the end of inflation), regardless of continuous entropy production, the final yield of DM is expected to be larger than the corresponding value obtained in UV freeze-in in the RD scenario with the same reheat temperature. To make a proper comparison between these two cases, for a given WI model and its corresponding temperature evolution, we define the reheat temperature, T_{rh} , as the temperature of the bath once the Universe enters the RD phase, i.e. $T_{\text{rh}} \equiv T(\epsilon_H = 2)$ where $\epsilon_H \equiv -\dot{H}/H^2$. Then, we introduce $R_\chi^{(n)}$:

$$R_\chi^{(n)} \equiv Y_{\chi,\infty} / Y_{\chi,\infty}^{\text{RD}}(T_{\text{rh}}), \quad (10)$$

as the ratio of $Y_{\chi,\infty}$, the final value of the yield obtained from Eqs. (5) and (6), to $Y_{\chi,\infty}^{\text{RD}}(T_{\text{rh}})$, evaluated from Eq. (9).

By taking the limit of the semi-analytical expression for the yield given by Eq. (8) when $N_e \rightarrow \infty$, we can simply estimate $R_\chi^{(n)}$ as:

$$R_\chi^{(n)} \simeq (2n-1) \frac{\mathcal{I}_\chi(N_e^{\text{peak}})}{\mathcal{I}_\chi(N_e^{\text{RD}})} \Delta N_e^{\text{peak}}, \quad (11)$$

where N_e^{RD} corresponds to the e-fold at which the Universe becomes RD, i.e. $N_e^{\text{RD}} \equiv N_e(\epsilon_H = 2)$, or equivalently, $T(N_e^{\text{RD}}) = T_{\text{rh}}$. Due to the sharp peak characteristic of \mathcal{I}_χ , the ratio $\mathcal{I}_\chi(N_e^{\text{peak}})/\mathcal{I}_\chi(N_e^{\text{RD}})$ is always $\gg 1$. Consequently, as the other contributing factors in Eq. (11) are individually > 1 , it follows generically that $R_\chi^{(n)} \gg 1$, i.e. UV freeze-in production of DM in WI is always enhanced compared to the one in a RD phase. This enhancement increases noticeably by increasing n which is attributed mainly to two distinct effects that it has on the ratio $\mathcal{I}_\chi(N_e^{\text{peak}})/\mathcal{I}_\chi(N_e^{\text{RD}})$. First, for a larger n , there is a faster decay of \mathcal{I}_χ after its peak. This implies that, for a fixed distance from the peak, $N_e^{\text{RD}} - N_e^{\text{peak}}$, the value of \mathcal{I}_χ at N_e^{RD} decreases relative to $\mathcal{I}_\chi(N_e^{\text{peak}})$

as n increases. Second, for a larger n , \mathcal{I}_χ reaches its peak at an earlier time, causing the onset of the RD phase, i.e. N_e^{RD} , to move further away from the peak, additionally contributing to the enhancement of the ratio $\mathcal{I}_\chi(N_e^{\text{peak}})/\mathcal{I}_\chi(N_e^{\text{RD}})$.

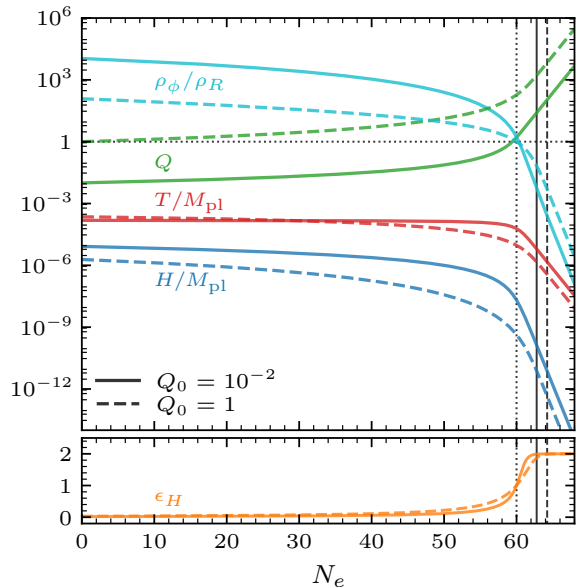


FIG. 1. The evolution of various quantities for the case of WI with $V(\phi) = \lambda\phi^4$ as a function of the number of e-folds after the onset of inflation, for two initial values of the dissipation strength $Q \equiv \Upsilon/(3H)$, namely 10^{-2} (solid lines) and 1 (dashed lines). The *top panel* presents the evolution of the bath temperature T (red), the Hubble rate H (blue), the dissipation strength Q (green) and the inflaton to radiation energy density ratio of ρ_ϕ/ρ_R (cyan). The *bottom panel* tracks the Hubble slow-roll parameter $\epsilon_H \equiv -\dot{H}/H^2$. In both examples, we set the parameters of the inflaton potential such that inflation ends after 60 e-folds (marked by the dotted vertical line) and its observables are consistent with CMB data. The onset of radiation domination corresponds to $\epsilon_H = 2$ and is also marked in the figure by a vertical line (respectively solid and dashed for $Q_0 = 10^{-2}$ and $Q_0 = 1$).

A Representative Example.— To illustrate the efficiency and richness of this novel mechanism, let us consider as an example the case of a quartic inflaton potential $V(\phi) = \lambda\phi^4$ and a linear dissipation rate $\Upsilon \propto T$. This is motivated by the inflationary model dubbed Warm Little Inflaton [14, 15], which constitutes the simplest successful realization of WI, in agreement with the cosmic microwave background (CMB) data for a large portion of its parameter space (unlike cold inflation with a quartic potential which is ruled out [16]).

Central to our analysis is the effectiveness at which the inflaton converts into radiation, typically parameterized by the dimensionless parameter:

$$Q \equiv \Upsilon/(3H). \quad (12)$$

We specifically consider two representative scenarios with initial dissipation strength equal to $Q_0 = 10^{-2}$ and

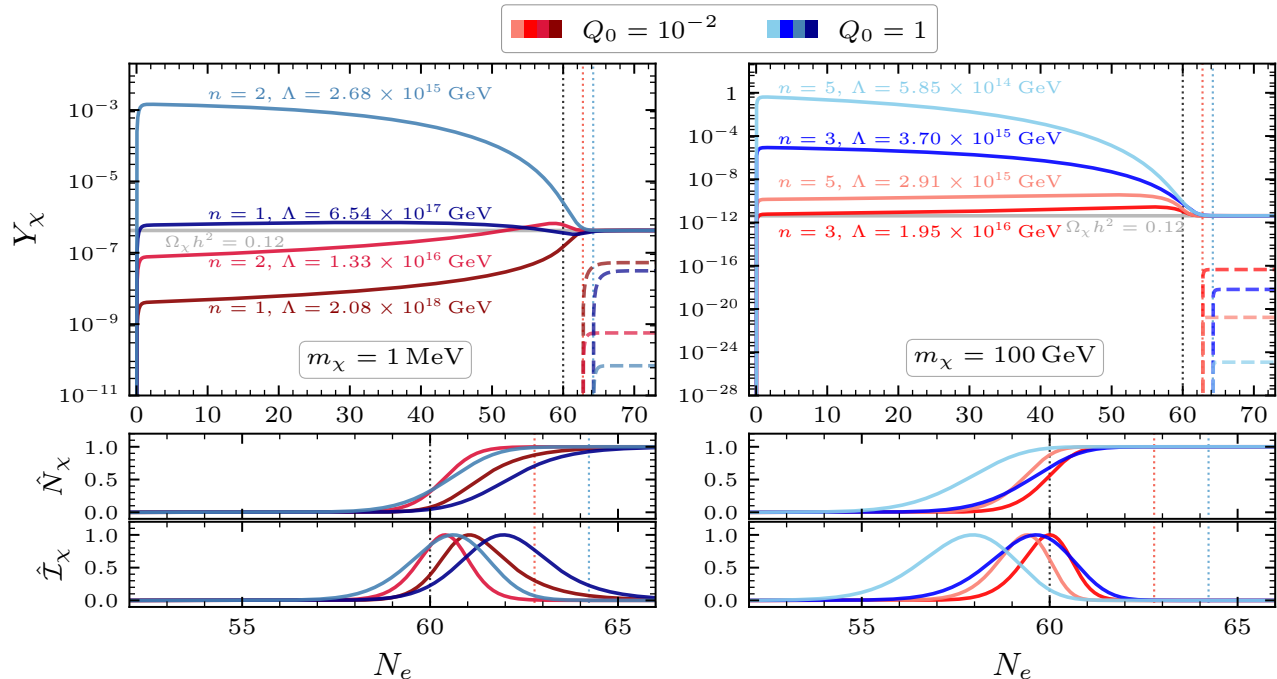


FIG. 2. *Top:* The DM yield Y_χ (solid lines) as a function of the number of e-folds after the onset of inflation, where the three dotted vertical lines mark the end of inflation (in black, here at $N_e = 60$) and the onset of RD phase for the two WI scenarios under consideration (in red for $Q_0 = 10^{-2}$ and blue for $Q_0 = 1$). The results shown here assume vanishing initial DM abundance and use the quantities shown in Fig. 1 for $Q_0 = 10^{-2}$ (red) and $Q_0 = 1$ (blue). In each case, we show the resulting yield for various values of the parameter n (introduced in Eq. (4)), with the DM mass m_χ and the scale Λ fixed to match the observed DM relic abundance, $\Omega_\chi h^2 = 0.12$ (solid grey line). Specifically, on the left (right) panel, we take $m_\chi = 1$ MeV ($m_\chi = 100$ GeV) and show the cases $n = \{1, 2\}$ ($n = \{3, 5\}$). In both panels (towards the right side), the dashed lines represent the corresponding yield evolution in the conventional RD UV freeze-in, i.e. assuming no DM yield prior to the onset of the RD phase. One can see the pronounced enhancement in DM yield achieved in WIFI relative to the conventional RD scenario, emphasizing how both the exponent n and the specific WI dynamics, represented by the choices of $Q_0 = 10^{-2}$ and $Q_0 = 1$, critically influence the yield. *Bottom:* The comoving DM number density $N_\chi \equiv e^{3N_e} n_\chi$ and its derivative $\mathcal{I}_\chi = dN_\chi/dN_e$, see also Eq. (6), corresponding to the yield evolution in the top panel and scaled so that their maximum equals 1 (represented by a hat symbol). These two lower panels elucidate the key e-folds around the peak of \mathcal{I}_χ during which the bulk of the DM production occurs. They explicitly show that within our framework the DM relic abundance is consistently established before the onset of the RD epoch. For sufficiently large values of n , essentially all of the DM in the Universe can be created during the inflationary phase itself.

$Q_0 = 1$. In both cases, we assume 60 e-folds of inflation, the Standard Model (SM) value for $g_\star = 106.75$,⁴ and set the height of the potential in order to produce cosmological observables consistent with CMB observations. To be specific, we take $N_e = 0$, i.e. 60 e-folds before the end of inflation, to correspond to the horizon crossing of the relevant CMB modes, and evaluate accordingly the amplitude of the scalar power spectrum $\Delta_{\mathcal{R}}^2$, its spectral index n_s and the tensor-to-scalar ratio r [17].⁵ Fixing the self-interacting quartic coupling λ to 1.15×10^{-15}

(7.91×10^{-16}) yields $\Delta_{\mathcal{R}}^2 = 2.1 \times 10^{-9}$, $n_s \simeq 0.967$ ($n_s \simeq 0.968$) and $r \simeq 7.6 \times 10^{-3}$ ($r \simeq 3.9 \times 10^{-4}$) for $Q_0 = 10^{-2}$ ($Q_0 = 1$), in agreement with the bounds set by the *Planck* collaboration [16].

In Fig. 1, we illustrate the cosmological dynamics for these two examples. As expected, the inflaton potential energy dominates the energy balance throughout the inflationary phase, while sustaining a radiation bath with nearly constant temperature above the corresponding Hubble rate. In both cases, the dissipation becomes strong ($Q > 1$) towards the end of inflation, allowing for the radiation to smoothly take over as the dominant component within roughly 2 (4) e-folds after the end of

⁴ Note, g_\star is technically determined by the underlying microphysical WI construction of interest. However, its value does not change our results qualitatively (see for instance Eq. (11)), hence we set it to its natural SM value.

⁵ Setting the number of e-folds at which observable scales cross the horizon to 60 effectively imposes the scale of the inflaton

potential to be roughly $\sim 10^{16}$ GeV [18, 19]. This assumption is consistent with the scenarios presented in this *letter*.

inflation for $Q_0 = 10^{-2}$ ($Q_0 = 1$). Following this transition, both the temperature and Hubble rate settle into their standard RD Universe evolution, i.e. $T \sim e^{-N_e}$ and $H \sim T^2$.

Our main results are illustrated in Fig. 2. On the top panel of the figure, we present the full evolution of the DM yield for $Q_0 = 10^{-2}$ and $Q_0 = 1$, depicted in varying shades of red and blue respectively, each corresponding to different values of n . For all individual cases analyzed, solid lines represent the evolution assuming a vanishing abundance at the start of inflation, and matched to the observed DM relic abundance of $\Omega_{\text{CDM}} h^2 = 0.12$ [20]. Dashed lines instead depict the corresponding DM yield evolution under the assumption of a vanishing abundance at the onset of the RD epoch. Specifically, on the left (right) panel, we take $m_\chi = 1$ MeV ($m_\chi = 100$ GeV) and show the cases $n = \{1, 2\}$ ($n = \{3, 5\}$).

Notably, across all the cases analyzed here, the DM relic abundance obtained from the full background evolution (including the inflationary phase) is always significantly greater than the corresponding yield from the subsequent RD era. Specifically, the enhancement is at least 1 order of magnitude and it increases exponentially with the value of n , corroborating to the general conclusions established in the previous section, i.e. Eq. (11). In addition, we also note that the enhancement in the DM yield is consistently higher for $Q_0 = 1$ compared to $Q_0 = 10^{-2}$. This can be understood from the sharper temperature drop near the end of inflation and longer transition to RD phase of the $Q_0 = 1$ case, as evidenced in Fig.1. These factors cause an earlier peak in \mathcal{I}_χ and an increased distance between this peak and the onset of RD phase, thereby leading to a higher enhancement ratio $R_\chi^{(n)}$ for $Q_0 = 1$ relative to $Q_0 = 10^{-2}$.

The insights gained from the top panel of Fig. 2 are further elucidated in its lower panels, which illustrate the corresponding evolution of the comoving DM number density N_χ and its derivative \mathcal{I}_χ (Eq.(6)), both scaled so that their maximum is one. These plots effectively highlight the time interval in which the bulk of DM production occurs for all of the examples under consideration. From the figure, we observe that the critical increase in N_χ always occurs at the peak of \mathcal{I}_χ , and within just a few e-folds around it. In all cases, the relic value of N_χ is predominantly established before the RD epoch, which demonstrates why our mechanism consistently leads to an enhancement in DM abundance compared to the RD UV freeze-in. Furthermore, the panel showing the \mathcal{I}_χ evolution visually confirms our expectation that a greater enhancement in DM yield will correspond to a larger gap between the peak of \mathcal{I}_χ and the onset of the RD phase. This explains the more pronounced boost in DM production with increasing values of n , as well as the amplification for the $Q_0 = 1$ case over $Q_0 = 10^{-2}$. Of particular interest is the behavior for the largest n values analyzed here, specifically within the $Q_0 = 1$ scenario. In these instances, we observe that essentially all of the DM is produced during the inflationary phase itself, leading to

the greatest enhancement in DM yield relative to the RD UV freeze-in. The possibility of producing all of the DM in the Universe during the inflationary period itself is a novel consequence of the WIFI scenario.

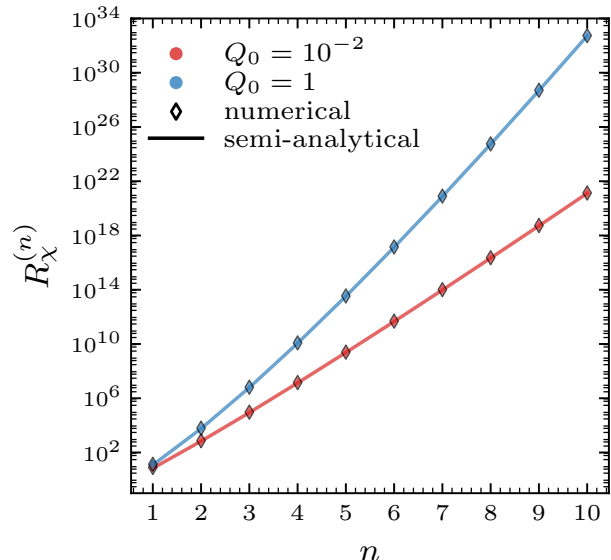


FIG. 3. The enhancement ratio $R_\chi^{(n)}$, as defined in Eq. (10), plotted as a function of the exponent n in the non-renormalizable interaction between DM and the bath, for the two WI scenarios with $Q_0 = 10^{-2}$ (red) and $Q_0 = 1$ (blue), each featuring a quartic inflaton potential and a temperature-linear dissipation rate. This panel presents both the numerical results (diamonds) and the corresponding semi-analytical estimates (solid lines), see Eq. (11), showing the close agreement between the two. More importantly, the figure vividly illustrates the exponential increase of $R_\chi^{(n)}$ with n , highlighting the remarkable enhancement of DM yield in WIFI compared to the RD scenario for the same reheat temperature, especially for large values of n .

Building on these observations, Fig. 3 illustrates the potentially enormous efficacy of DM production via WIFI. In this figure, the enhancement ratio $R_\chi^{(n)}$, as defined by Eq. (10), is plotted as a function of n for both scenarios: $Q_0 = 10^{-2}$ (red) and $Q_0 = 1$ (blue). The numerical evaluations of $R_\chi^{(n)}$ are shown as diamonds, while our semi-analytical estimates, Eq. (11), are represented by solid lines. As anticipated, $R_\chi^{(n)}$ is always greater than one and it increases exponentially with the value of n . Specifically, $R_\chi^{(n)} \gg 10^3$ for all $n \geq 3$ and can be as large as $\sim 10^{20}$ ($\sim 10^{30}$) for $n = 10$ and $Q_0 = 10^{-2}$ ($Q_0 = 1$). This underscores the remarkable efficiency of DM production from WIFI, far surpassing the yield from the conventional RD epoch subsequent to WI. In addition, the consistently larger values of $R_\chi^{(n)}$ for the $Q_0 = 1$ scenario compared to $Q_0 = 10^{-2}$ emphasize the substantial impact of the specific WI dynamics on the overall enhancement in DM yield within our framework. In all of these cases, our semi-analytical estimates match

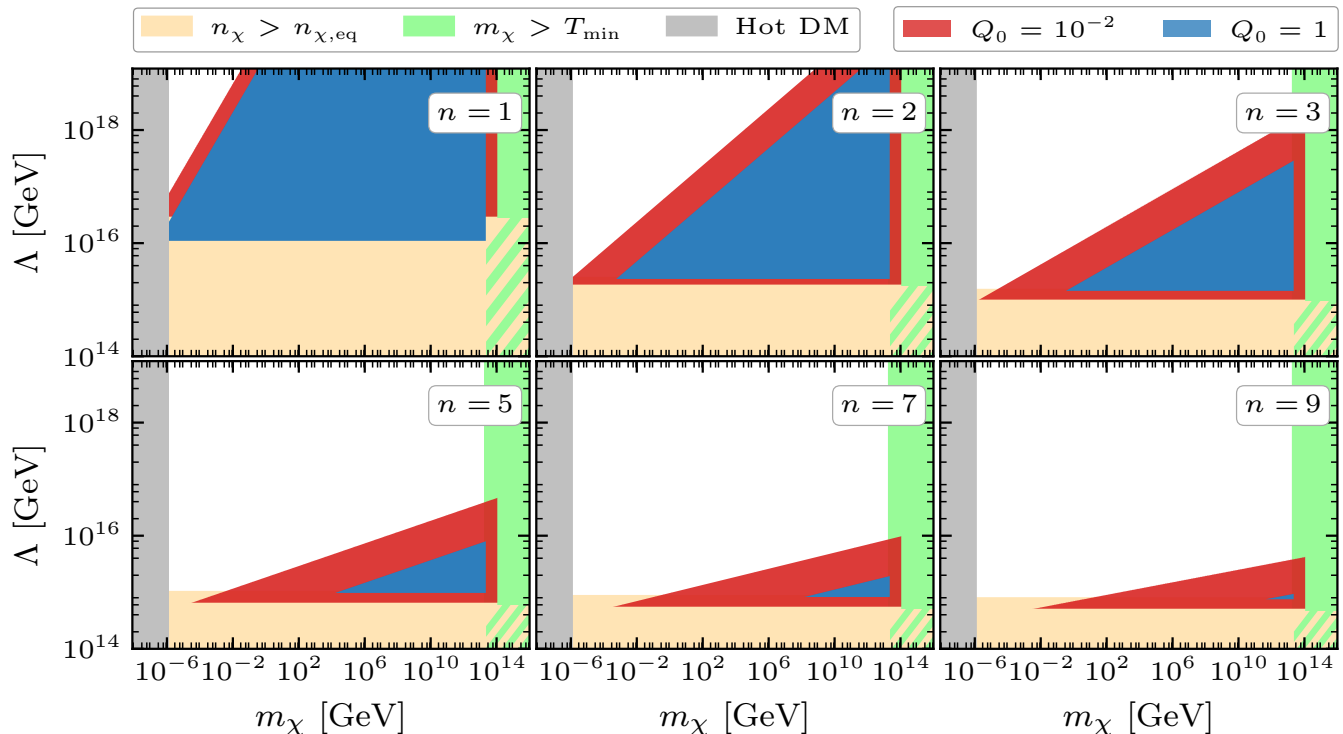


FIG. 4. Constraints on DM production from WIFI in the (m_χ, Λ) plane, with m_χ denoting the DM mass and Λ representing the scale of the non-renormalizable operator connecting DM with the bath, Eq. (4). Displayed in separate panels for $n = \{1, 2, 3, 5, 7, 9\}$, where n indicates the exponent in the non-renormalizable interaction. The gray, yellow, and green shaded areas are excluded by structure formation, the requirement that DM does not come in to thermal equilibrium with the bath, and the temperature of the radiation respectively. Within the red and the blue shaded regions, DM is overproduced ($\Omega_\chi > \Omega_{\text{CDM}}$) for the WI scenarios with $Q_0 = 10^{-2}$ and $Q_0 = 1$, respectively, each featuring a quartic inflaton potential and a temperature-linear dissipation rate. Here, Ω_{CDM} stands for the observed (cold) DM abundance.

the numerical evaluations of $R_\chi^{(n)}$ well, with discrepancies consistently below 15%, indicating the reliability of our semi-analytical description in capturing the complex dynamics of DM production in WI.

Overall, given this analysis, it may seem that higher dissipation strength Q always leads to a greater enhancement in DM yield. While this trend holds for scenarios with a monomial potential and a dissipation rate linear in temperature, it should not be considered a universal rule across all WI constructions. The interplay between the potential type and the form of the dissipation rate can yield complex outcomes, warranting further investigation to fully understand these dynamics.

Lastly, it is important to comment on the allowed DM mass range. Beyond the simple upper bound on m_χ set by the minimum temperature sustained by the bath, matching the DM relic abundance introduces a notable degeneracy between the scale Λ , the exponent n of the non-renormalizable operator, and m_χ . Further considerations within our framework, namely the requirement that DM is cold and never reaches thermal equilibrium with the bath, narrow down the viable parameter space. As a result, the minimum DM mass required to match the observed abundance today tends to increase with the

value of n , reflecting the nuanced interplay between Λ , n and m_χ within our framework. This dependency is strongly influenced by the specific WI scenario. We illustrate this explicitly in Fig. 4 where we plot the interrelation of Λ , n and m_χ for the $Q_0 = 10^{-2}$ (red region) and $Q_0 = 1$ (blue region) scenarios with $n \in \{1, 2, 3, 5, 7, 9\}$, and assuming one degree of freedom for χ : $g_\chi = 1$. This depiction clearly differentiates the viable parameter space for each scenario, underscoring their extensive range and uniqueness.

Discussion and Summary. — In this *letter*, we have introduced a novel perspective on the role of inflation in the thermal production of DM via freeze-in. We demonstrated that in a WI setting the persistent thermal bath, sustained by the dissipative interactions with the inflaton field, can source a sizable DM abundance via the non-renormalizable interaction characteristic of UV freeze-in, Eq (4). Compared to the (conventional) RD UV freeze-in scenario for the same reheat temperature, the resulting DM yield in WIFI is always enhanced, showing a strongly positive dependence on the exponent n of the non-renormalizable operator, see Eq. (11). We further explored the robustness of DM production in WIFI through a physically-motivated WI model, characterized

by a quartic potential, a temperature-linear dissipation rate, and two parameter choices for the initial dissipation strength, namely $Q_0 = 10^{-2}$ and $Q_0 = 1$. These examples explicitly illustrate the efficacy of DM freeze-in from WI, as well as the significant influence of the specific WI dynamics on the overall enhancement in DM yield, see Figs. 2 and 3. Notably, for sufficiently large values of n , the DM relic abundance is entirely created during the inflationary phase, leading to an enhancement in DM yield relative to the RD UV freeze-in that reaches up to 20 (30) orders of magnitude for the $Q_0 = 10^{-2}$ ($Q_0 = 1$) scenario. This new central role of the inflationary phase in the DM production highlights a key distinction of our mechanism from RD UV freeze-in: in WIFI, the relic DM yield is mostly determined by the specific period where the interplay of the bath temperature and Hubble parameter fulfills Eq. (7), rather than by the highest temperature of the bath alone.

Furthermore, the WIFI mechanism proposed in this *letter* emerges as a natural extension of the WI framework. In fact, most WI constructions generate a bath of beyond the SM particles rather than the SM ones [14, 21–24]. In these cases, it is then necessary to introduce new particles and interactions to eventually produce the SM. Our framework leverages this by considering one of these new fields as DM, interacting with the radiation through

heavy mediators. This not only underscores the generality of our findings within the WI setting but also suggests a broader applicability. The mechanism we have explored here for DM production can be instead used to produce other relics, which could potentially play a significant role in the early Universe evolution. In summary, our work provides a foundation for exploring a range of cosmological phenomena relevant for DM production and beyond, within the versatile framework of WI. We leave the study and exploration of concrete model realizations to future work.

Acknowledgments.— K.F. is Jeff & Gail Kodosky Endowed Chair in Physics at the University of Texas at Austin, and K.F. and G.M. are grateful for support via this Chair. K.F. G.M. and B.S.E. acknowledge support by the U.S. Department of Energy, Office of Science, Office of High Energy Physics program under Award Number DE-SC-0022021. K.F. and G.M. also acknowledge support from the Swedish Research Council (Contract No. 638-2013-8993). The authors would like to thank the Leinweber Center for Theoretical Physics, University of Michigan, for hospitality while this work was being completed. We acknowledge the use of WarmSPy [17], and the Python packages Matplotlib [25], Numpy [26] and Scipy [27].

-
- [1] L. J. Hall, K. Jedamzik, J. March-Russell, and S. M. West, *JHEP* **03**, 080 (2010), arXiv:0911.1120 [hep-ph].
- [2] F. Elahi, C. Kolda, and J. Unwin, *JHEP* **03**, 048 (2015), arXiv:1410.6157 [hep-ph].
- [3] D. J. H. Chung, E. W. Kolb, and A. Riotto, *Phys. Rev. D* **60**, 063504 (1999), arXiv:hep-ph/9809453.
- [4] G. F. Giudice, E. W. Kolb, and A. Riotto, *Phys. Rev. D* **64**, 023508 (2001), arXiv:hep-ph/0005123.
- [5] E. W. Kolb, A. Notari, and A. Riotto, *Phys. Rev. D* **68**, 123505 (2003), arXiv:hep-ph/0307241.
- [6] M. A. G. Garcia, Y. Mambrini, K. A. Olive, and M. Peloso, *Phys. Rev. D* **96**, 103510 (2017), arXiv:1709.01549 [hep-ph].
- [7] S.-L. Chen and Z. Kang, *JCAP* **05**, 036 (2018), arXiv:1711.02556 [hep-ph].
- [8] N. Bernal, F. Elahi, C. Maldonado, and J. Unwin, *JCAP* **11**, 026 (2019), arXiv:1909.07992 [hep-ph].
- [9] B. Barman, N. Bernal, Y. Xu, and O. Zapata, *JCAP* **07**, 019 (2022), arXiv:2202.12906 [hep-ph].
- [10] M. A. G. Garcia and M. A. Amin, *Phys. Rev. D* **98**, 103504 (2018), arXiv:1806.01865 [hep-ph].
- [11] A. Berera, *Phys. Rev. Lett.* **75**, 3218 (1995), arXiv:astro-ph/9509049.
- [12] A. Berera and L.-Z. Fang, *Phys. Rev. Lett.* **74**, 1912 (1995), arXiv:astro-ph/9501024.
- [13] A. Berera, M. Gleiser, and R. O. Ramos, *Phys. Rev. Lett.* **83**, 264 (1999), arXiv:hep-ph/9809583.
- [14] M. Bastero-Gil, A. Berera, R. O. Ramos, and J. G. Rosa, *Phys. Rev. Lett.* **117**, 151301 (2016), arXiv:1604.08838 [hep-ph].
- [15] M. Bastero-Gil, A. Berera, R. O. Ramos, and J. G. Rosa, *Phys. Lett. B* **813**, 136055 (2021), arXiv:1907.13410 [hep-ph].
- [16] Y. Akrami *et al.* (Planck), *Astron. Astrophys.* **641**, A10 (2020), arXiv:1807.06211 [astro-ph.CO].
- [17] G. Montefalcone, V. Aragam, L. Visinelli, and K. Freese, *JCAP* **01**, 032 (2024), arXiv:2306.16190 [astro-ph.CO].
- [18] A. R. Liddle and S. M. Leach, *Phys. Rev. D* **68**, 103503 (2003), arXiv:astro-ph/0305263.
- [19] G. Montefalcone, V. Aragam, L. Visinelli, and K. Freese, *JCAP* **03**, 002 (2023), arXiv:2212.04482 [gr-qc].
- [20] N. Aghanim *et al.* (Planck), *Astron. Astrophys.* **641**, A6 (2020), [Erratum: *Astron. Astrophys.* 652, C4 (2021)], arXiv:1807.06209 [astro-ph.CO].
- [21] A. Berera, I. G. Moss, and R. O. Ramos, *Rept. Prog. Phys.* **72**, 026901 (2009), arXiv:0808.1855 [hep-ph].
- [22] A. Berera and R. O. Ramos, *Phys. Lett. B* **567**, 294 (2003), arXiv:hep-ph/0210301.
- [23] I. G. Moss and C. Xiong, (2006), arXiv:hep-ph/0603266.
- [24] K. V. Berghaus, P. W. Graham, and D. E. Kaplan, *JCAP* **03**, 034 (2020), arXiv:1910.07525 [hep-ph].
- [25] J. D. Hunter, *Computing in Science and Engineering* **9**, 90 (2007).
- [26] C. R. Harris *et al.*, *Nature* **585**, 357 (2020), arXiv:2006.10256 [cs.MS].
- [27] P. Virtanen *et al.*, *Nature Methods* **17**, 261 (2020), arXiv:1907.10121 [cs.MS].